

## MIT Open Access Articles

*Impaired Hippocampal Ripple-Associated  
Replay in a Mouse Model of Schizophrenia*

The MIT Faculty has made this article openly available. **Please share**  
how this access benefits you. Your story matters.

**Citation:** Suh, Junghyup, David J. Foster, Heydar Davoudi, Matthew A. Wilson, Susumu Tonegawa. "Impaired Hippocampal Ripple-Associated Replay in a Mouse Model of Schizophrenia." *Neuron* 80, (2013) pp. 484–493.

**As Published:** <http://dx.doi.org/10.1016/j.neuron.2013.09.014>

**Publisher:** Elsevier/Cell Press

**Persistent URL:** <http://hdl.handle.net/1721.1/102677>

**Version:** Author's final manuscript: final author's manuscript post peer review, without publisher's formatting or copy editing

**Terms of use:** Creative Commons Attribution-NonCommercial-NoDerivs License



Published in final edited form as:

*Neuron*. 2013 October 16; 80(2): . doi:10.1016/j.neuron.2013.09.014.

## Impaired hippocampal ripple-associated replay in a mouse model of schizophrenia

Junghyup Suh<sup>1,2,\*</sup>, David J. Foster<sup>2,3,\*</sup>, Heydar Davoudi<sup>4</sup>, Matthew A. Wilson<sup>2</sup>, and Susumu Tonegawa<sup>1,2</sup>

<sup>1</sup>RIKEN-MIT Center for Neural Circuit Genetics, Massachusetts Institute of Technology, 77 Massachusetts Avenue, Cambridge, MA 02139

<sup>2</sup>The Picower Institute for Learning and Memory, Department of Biology and Department of Brain and Cognitive Sciences, Massachusetts Institute of Technology, 77 Massachusetts Avenue, Cambridge MA 02139

<sup>3</sup>Solomon H. Snyder Department of Neuroscience, Johns Hopkins University School of Medicine, 725 N. Wolfe Street, Baltimore MD 21205

<sup>4</sup>Department of Biomedical Engineering, Johns Hopkins University School of Medicine, 720 Rutland Avenue, Baltimore MD 21205

### SUMMARY

The cognitive symptoms of schizophrenia presumably result from impairments of information processing in neural circuits. We recorded neural activity in the hippocampus of freely behaving mice with a forebrain-specific knockout of the synaptic plasticity-mediating phosphatase calcineurin, that were previously shown to exhibit behavioral and cognitive abnormalities, recapitulating the symptoms of schizophrenia. Calcineurin knockout (KO) exhibited a 2.5-fold increase in the abundance of sharp-wave ripple (SWR) events during awake resting periods and single units in KO were overactive during SWR events. Pairwise measures of unit activity, however, revealed that the sequential reactivation of place cells during SWR events was completely abolished in KO. Since this relationship during the post-experience awake rest periods has been implicated in learning, working memory and subsequent memory consolidation, our findings provide a novel mechanism underlying impaired information processing, potentially resulting in the cognitive impairments in schizophrenia.

### Keywords

schizophrenia; hippocampus; replay; synaptic plasticity; calcineurin; animal model; sharp waves; ripples

© 2013 Elsevier Inc. All rights reserved.

Corresponding authors: Junghyup Suh, David J. Foster, junghyup@mit.edu, david.foster@jhu.edu.

\*These authors contributed equally to this work.

**Publisher's Disclaimer:** This is a PDF file of an unedited manuscript that has been accepted for publication. As a service to our customers we are providing this early version of the manuscript. The manuscript will undergo copyediting, typesetting, and review of the resulting proof before it is published in its final citable form. Please note that during the production process errors may be discovered which could affect the content, and all legal disclaimers that apply to the journal pertain.

## INTRODUCTION

Cognitive disorders such as schizophrenia are associated with multiple genetic and environmental factors, but presumably involve systematic impairments of information processing in specific neural circuits. Animal models can provide insight into such disorders by associating impairments at a behavioral level with disruption of distinct mechanisms at a neural circuit level (Arguello and Gogos, 2006). Furthermore, the ability to monitor the activity of individual neurons is a key advantage of using animal models. However, very little previous work has examined neural information processing in such models. In this study, we applied high-density electrophysiological recording techniques to investigate information processing at a circuit level in a mouse model of schizophrenia.

We previously generated a mouse model that offered three features: first, altered synaptic plasticity; second, a profile of behavioral impairments recapitulating those seen in schizophrenia patients; and third, an association of the mutated gene with schizophrenia (Gerber et al., 2003; Gerber and Tonegawa, 2004; Miyakawa et al., 2003; Zeng et al., 2001). Specifically, mice with a forebrain-specific knockout (KO) of the only regulatory subunit of calcineurin, a major phosphatase expressed in the brain, are severely deficient in long-term depression (LTD) at hippocampal synapses, while long-term potentiation (LTP) is mildly enhanced (Zeng et al., 2001), leading to a leftward shift in the BCM curve (Dudek and Bear, 1992). The KO mice exhibit a comprehensive array of behavioral impairments characteristic of schizophrenia patients (Elvevag and Goldberg, 2000; Goldman-Rakic, 1994), including impairments in latent inhibition, pre-pulse inhibition and social interaction (Miyakawa et al., 2003), as well as a severe deficit in working memory (Zeng et al., 2001). Furthermore, the mutated calcineurin gene (*PPP3CC*) has been shown to map to chromosomal loci previously implicated in schizophrenia by genetic linkage studies (Gerber et al., 2003). Taken together, these features suggest that the calcineurin KO provides a unique opportunity to investigate the neural basis of dysfunction in a schizophrenia model.

The hippocampus is a brain structure critical for episodic memory (Gaffan, 1994; Olton and Samuelson, 1976; Scoville and Milner, 1957; Steele and Morris, 1999) and spatial learning (Morris et al., 1982; O'Keefe and Nadel, 1978). In freely moving rodents, the hippocampus exhibits distinct activity profiles dependent on behavioral state (Buzsaki, 1989), suggesting distinct modes of information processing within the structure. During running, the hippocampal electroencephalogram (EEG) exhibits a 4–12 Hz theta rhythm (Skaggs et al., 1996), and hippocampal principal neurons exhibit location-specific responses, known as place fields, as reported in rats (O'Keefe and Dostrovsky, 1971), mice (McHugh et al., 1996), monkeys (Matsumura et al., 1999) and humans (Ekstrom et al., 2003). By contrast, during awake rest periods, hippocampal EEG is distinguished by sharp-wave-ripple (SWR) events (Buzsaki, 1989) and hippocampal principal neurons take part in extended sequences of coactivity, which replay previous behavioral episodes (Davidson et al., 2009; Diba and Buzsaki, 2007; Foster and Wilson, 2006; Gupta et al., 2010) as well as preplay subsequent behavioral episodes (Dragoi and Tonegawa, 2011; Dragoi and Tonegawa, 2013; Pfeiffer and Foster, 2013).

There is substantial evidence linking schizophrenia with damage to the hippocampus (Weinberger, 1999). Dysfunction of the hippocampus and related medial temporal lobe structures has also been reported in schizophrenia patients (Small et al., 2011), together with selective impairments in learning and memory. In addition, abnormal brain activity in schizophrenia patients was detected in various brain structures, including the hippocampus, during rest periods (Buckner et al., 2008) and during passive task epochs (Harrison et al., 2007). Since the pattern of impairments of calcineurin KO mice – synaptic plasticity changes in the hippocampus and hippocampal-dependent behavioral phenotypes such as

working memory – suggested that hippocampal function might be affected in this mouse model of schizophrenia, we targeted the hippocampus for electrophysiological recordings in freely behaving KO and littermate controls (CT) and investigated changes in information processing during exploratory behavior and resting periods.

## RESULTS

To characterize hippocampal activity in our mouse model, we employed microdrives with multiple independently adjustable tetrodes to record single-unit spikes and EEG from the CA1 subregion of the dorsal hippocampus of freely behaving KO mice ( $N = 7$ ) and floxed littermate CT ( $N = 5$ ).

### Overabundance of SWR in calcineurin KO mice

We hypothesized that the bias toward enhanced synaptic strength in KO would lead to an increase in excitability in hippocampal circuits. We therefore analyzed hippocampal EEG in KO and CT during both running and awake non-exploratory periods. During immobility, both groups exhibited SWRs, defined as increases in amplitude in the ripple frequency band (100–240 Hz), and typically lasting up to hundreds of milliseconds (Figure 1A). However, the non-Z-scored EEG in KO exhibited a significant increase in ripple power compared to CT (Mann-Whitney,  $p < 0.05$ ; Figure 1B). By contrast, there was no increase in power in either the gamma band (25–80 Hz; Mann-Whitney, NS; Figure 1C) during non-exploratory period or theta band (4–12 Hz; Mann-Whitney, NS; Figure 1D) frequency during run.

To investigate further the specific increase in ripple-related activity, we quantified the characteristics of SWR events. No change was found in the duration (CT:  $88.35 \pm 3.6$  ms; KO:  $88.36 \pm 2.42$  ms;  $F(1, 10) = 1.17e^{-5}$ , NS) or Z-scored amplitude (CT:  $7.06 \pm 0.32$  sd; KO:  $7.72 \pm 0.12$  sd;  $F(1, 10) = 4.8$ , NS) of SWRs. The abundance of SWRs, however, was 2.5 times greater ( $F(1,10) = 31.7$ ,  $p < 0.001$ ; Figure 1E). We then varied our analysis parameters in order to test how robust the results were. Varying the SWR detection threshold, in standard deviations from the mean, we found a consistent effect as the amplitude threshold was increased (Figure 1F). Indeed, at 8 standard deviations, the number of SWRs was a full order of magnitude greater in KO than CT. We further conducted a robustness analysis varying the frequency range for which events were defined, for a 50 ms window, varied from 50 Hz to 600 Hz in 10 Hz steps (Figure 1G). There were significantly more events over a wide range of frequencies, between 100 Hz and 480 Hz (all windows in the range were significant at  $p < 0.05$ , two-sample t-test), however, the most significant zone was between 120 Hz and 150 Hz (all windows in this range were significant at  $p < 0.001$ , two-sample t-test). This range matched the frequency of peak ripple power (CT:  $149.8 \pm 5.3$  Hz; KO:  $143.4 \pm 4.4$  Hz;  $F(1,10) = 0.83$ , NS; Figure 1B). Taken together, these results indicate that calcineurin KO exhibit higher excitability in the EEG during immobility, whereas EEG activity associated with active exploration does not appear to be affected.

### Normal place fields in calcineurin KO during exploratory behavior

Across multiple species, hippocampal pyramidal neurons are active in spatially restricted regions of an environment during exploration, a pattern of activity referred to as place fields (Ekstrom et al., 2003; Matsumura et al., 1999; McHugh et al., 1996; O'Keefe and Dostrovsky, 1971; Wilson and McNaughton, 1993). Given the great increase in ripple activity in the EEG during rest periods and the overall shift in synaptic plasticity toward potentiation (Zeng et al., 2001), we next hypothesized that higher excitability in KO may be manifested in the activity of individual neurons. We therefore isolated single unit activity in large numbers of pyramidal neurons simultaneously recorded from CA1 during running (Total cells: CT:  $N = 59$ , KO:  $N = 122$ ; simultaneously: CT:  $11.8 \pm 1.0$  cells per mouse; KO:

17.4  $\pm$  2.1 cells per mouse; Figure 2A) and analyzed units (CT:  $N = 48$ ; KO:  $N = 92$ ) with significant activity on the track (place field peak  $> 1$ Hz). Fine quantification revealed no differences in these responses across multiple measures (Figure 2; See also Figure S1). Specifically, single units in KO exhibited normal place field sizes ( $F(1,138) = 0.01$ , NS; Figure 2B), normal firing rates within place fields ( $F(1,138) = 0.56$ , NS; Figure 2C), no difference in the normal tendency of units to fire more in one direction than another ( $F(1,138) = 0.19$ , NS; Figure 2D), and no difference in sparsity ( $F(1,138) = 0.85$ , NS; Figure 2E), which is a measure of the localization of place fields (Jung et al., 1994). In addition, no difference was observed in spatial information index ( $F(1,138) = 0.02$ , NS; Figure 2F), which measures how informative about position a spike from a place cell is (Markus et al., 1994), and spatial coherence ( $F(1,138) = 0.92$ , NS; Figure 2G), which measures the local smoothness of a firing rate pattern of spikes (Muller and Kubie, 1989).

Next, to determine whether excitability might be evident in the precise timing of single spikes, we further examined run-time unit activity on a finer timescale. Since hippocampal single units exhibit complex spikes, made up of a burst of several spikes occurring between 2–10 ms apart (Quirk and Wilson, 1999), we first measured the number of spikes during bursts. Both KO and CT units exhibited similar numbers of spikes per burst ( $F(1,142) = 0.01$ , NS; Figure 2H) and a similar percentage of burst spikes ( $F(1,142) = 0.40$ , NS; Figure 2I). Interestingly, however, we found that bursts in KO tended to be faster, as measured by burst inter-spike interval (CT:  $5.70 \pm 0.70$  ms; KO:  $4.99 \pm 0.78$  ms;  $F(1,142) = 29.16$ ,  $p < 10^{-6}$ ; Figure 2J), and extracellular spike amplitude attenuation, which is associated with complex spikes (Harris et al., 2001; Quirk and Wilson, 1999), was also increased in KO (CT:  $2.84 \pm 0.39$  %; KO:  $5.93 \pm 0.38$  %;  $F(1,142) = 31.36$ ,  $p < 10^{-6}$ ; Figure 2J). Taken together, these results indicated that the spatial representation at the level of single cells in KO appears to be preserved during exploratory behavior, in spite of the bias toward enhanced synaptic strength, with little change in spike timing during bursts.

### Overactivity of place cells in calcineurin KO during SWRs

Since the place responses of single units in calcineurin KO were largely normal during run, we next examined whether unit activity during immobile periods, specifically SWRs, was also unaltered. In both KO and CT mice, single units exhibited spikes during SWR events (Figure 3A). Place cells in KO, however, fired more than double the number of spikes during each SWR event as compared to those in CT (CT:  $1.11 \pm 0.14$  spikes per SWR; KO:  $2.56 \pm 0.54$  spikes per SWR;  $F(1,81) = 4.84$ ,  $p < 0.05$ ; Figure 3B). Given that SWR events were also more abundant in KO mice (Figure 1E), the increased spikes per SWR further increased excitability in KO mice during rest periods. Specifically, the separate effects of increased spiking activity in SWRs (spikes/ripple) and increased abundance of SWRs (ripples/second) jointly resulted in an increase in the overall number of SWR spikes fired during rest periods (spikes/second). Indeed, KO displayed a six-fold increase in the number of SWR spikes during rest periods compared to CT (CT:  $0.10 \pm 0.02$  spikes/s; KO:  $0.62 \pm 0.13$  spikes/s,  $F(1,78) = 13.40$ ,  $p < 0.0005$ ; Figure 3C).

In principle, this increase in spiking activity may not by itself imply an alteration in the organization of information during each SWR. For example, the patterns of spikes associated with SWRs might be preserved, while being both enhanced and more frequent. However, such a possibility requires that the identity of cells participating in SWRs would not be altered. Alternatively, overexcitability during SWRs might lead to a degradation of SWR-associated information. To address this issue, we further analyzed the participation of single units across different SWRs. We found that single units in KO participated in a significantly greater fraction of SWR events than CT, increasing from around a third of SWRs to over half (CT:  $35.39 \pm 3.44$  %; KO:  $54.47 \pm 4.00$  %;  $F(1,86) = 11.63$ ,  $p < 0.001$ ;

Figure 3D). This finding indicates that neurons in KO were active during more than the optimal number of SWR events, raising the possibility that spikes in KO may add noise rather than signal to SWR events. Therefore, we analyzed the coactivity of simultaneously recorded units during SWRs, and determined whether and how the information content of SWRs was affected in calcineurin KO.

### Abolished spatial information content of reactivation events in calcineurin KO

It has been demonstrated that awake SWR events are associated with temporally sequenced activity patterns of hippocampal place cells, referred to as “replay” due to the resemblance to spatial activity patterns in prior behavioral experience (Davidson et al., 2009; Diba and Buzsaki, 2007; Foster and Wilson, 2006; Gupta et al., 2010; Karlsson and Frank, 2009). It has also been shown that SWR events are associated with consolidation of previously encoded memory (Ego-Stengel and Wilson, 2010; Girardeau et al., 2009; Nakashiba et al., 2009), with encoding of a novel experience (Dragoi and Tonegawa, 2011; Dragoi and Tonegawa, 2013) and, more interestingly, with spatial working memory (Jadhav et al., 2012) and the planning of future behaviors (Pfeiffer and Foster, 2013). Therefore, we hypothesized that temporal sequences of place cells associated with SWRs in KO may be affected. Since sequential replay suggests a distinct relationship between pairs of simultaneously recorded place cells, in which the distance between the cells’ place fields (measured using their peaks) should correlate with the temporal spike separation between cells during SWRs (Karlsson and Frank, 2009), we applied this analysis to pairs of simultaneously recorded place cells in KO and CT mice. We first noted that mean inter-spike intervals between pairs of cells were significantly shorter in KO than CT (CT:  $82.58 \pm 7.32$  ms; KO:  $29.3 \pm 2.03$  ms;  $F(1,428)=80.46$ ,  $p < 10^{-17}$ ). This result is in accordance with the general increase in spike rates during SWRs noted earlier. We then considered the relationship between place field distance and temporal spike separation for pairs of cells. We created a representation of activity across the population by generating cross correlograms of spike trains during SWRs for each pair of cells, and then imaging each correlogram as a colorized row vector positioned on the y axis at a height corresponding to the distance between the place fields of those cells. When two or more correlograms occupied the same distance value, they were averaged together. In CT, this analysis revealed a distributed “V”-like pattern indicative of a replay-like relationship, as has been reported in rats (Karlsson and Frank, 2009) (Figure 4A, left). Strikingly, in contrast, the pattern was very different for KO, with a tight concentration around the null relative spike timing at all distances (Figure 4A, right).

Next, to verify whether the abnormal pattern in the correlogram in KO mice indicated a fundamentally disordered organization at the level of pairs of cells, we measured the mean temporal spike separation for each pair of cells, thus considering each pair of cells as a tuple of place field distance and mean spike separation (Figure 4B). There was a clear and significant positive correlation between place field distance and temporal spike separation in SWRs among cell pairs in CT ( $r = 0.21$ ,  $F=6.65$ ,  $p < 0.01$ ), indicating that hippocampal unit activity during SWRs conveyed temporally structured information about the spatial distance of place fields. By contrast, the relationship between cell pairs in KO was completely abolished ( $r = -0.007$ ,  $F=0.015$ , NS). We also further quantified these pairwise effects by binning the data into “close” and “far” categories on the basis of the distance between place fields in a pair. Specifically, pairs of cells with place field peaks less than 10 cm apart were categorized as “close”, whereas pairs of cells with place field peaks more than 40 cm apart were categorized as “far”. CT exhibited a strong difference between these categories ( $F(1,76)=8.94$ ,  $p < 0.01$ ; Figure 4C, left), whereas KO exhibited no difference at all ( $F(1,194)=0.22$ , NS; Figure 4C, right). Furthermore, in order to compare CT and KO, and assess the consistency of our findings across subjects, we analyzed the effects of genotype and condition (“close” versus “far”) on the temporal separation of SWR spikes, with subject



as a random factor nested within genotype (see Experimental Procedures). We found significant effects of genotype ( $F(1,201)=15.1$ ,  $p < 0.01$ ), condition ( $F(1,201)=8.15$ ,  $p < 0.02$ ) and the interaction between them ( $F(1,201)=7.36$ ,  $p < 0.02$ ), but no effect of subject ( $F(10,201)=2.0$ , NS) or interaction between subject and condition ( $F(7,201)=1.75$ , NS), thus demonstrating that KO and CT mice differed significantly and consistently across subjects. Finally, the correlation coefficients across individual mice were different between KO and CT (z-test,  $Z=2.15$ ,  $p < 0.05$ ), thus demonstrating that the relationship between place fields and spike times was consistently disrupted across KO mice.

Since the increased abundance of SWRs and increased number of spikes during SWRs can contribute to the abolished spatial information content in KO, we further repeated the above analyses under three control-matching manipulations (for conciseness, we state only the interaction between genotype and condition, and the comparison of correlation coefficients). First, to exclude the possibility of the effect of the increase in spike numbers in KO having an effect, we randomly decimated spike numbers from spike trains to match their average quantity equal to CT spikes (Figure 4D; 3-way nested ANOVA,  $F(1)=5.21$ ,  $p < 0.05$  and z-test,  $Z=2.66$ ,  $p < 0.01$ ). Second, to exclude a possibility of the effect of the increase in SWR abundance in KO having an effect on abolished spatial information content, we randomly decimated the number of SWR events (Figure 4E; 3-way nested ANOVA,  $F(1)=7.74$ ,  $p < 0.05$  and z-test,  $Z=2.53$ ,  $p < 0.05$ ). Finally, we combined both decimations to analyze cell pairs in KO under the same SWR abundance and spike rates as CT (Figure 4F; 3-way nested ANOVA,  $F(1)=11.14$ ,  $p < 0.01$ , and z-test,  $Z=2.33$ ,  $p < 0.05$ ). In all three conditions, the two main factors were also significant, but the nested factor (subject) and its interaction with condition were not. Therefore, neither increased abundance nor increased spike rate by themselves account for the failure of cell pairs in KO to exhibit normally structured coactivity, but rather the fundamental relationship between spike times during SWRs and represented place fields during run has been completely abolished in KO.

## DISCUSSION

We applied high-density electrophysiology recording to a mouse model of schizophrenia, in which functional calcineurin protein is deleted specifically in excitatory neurons from the forebrain. Our primary aim was to detect disruption of information processing in the hippocampus, which may underlie the schizophrenia-like behavioral impairments of the model mice. We demonstrated that calcineurin KO mice displayed a selective disruption in rest-related neural information processing. Hippocampal EEG in KO exhibited enhanced power in the ripple band, but not gamma or theta, and a 2.5-fold increase in the abundance of SWR events during awake resting periods. This abnormality was strikingly selective, since CA1 neurons in KO exhibited normal place fields during active exploratory behavior. By contrast, the same neurons were profoundly overactive during SWRs and participated in a greater fraction of SWR events. Furthermore, pairwise measures of unit activity during SWRs revealed that a normal linear relationship between spatial separation of place fields during run and temporal separation of spikes during resting periods was completely abolished in KO. Thus, we present a novel form of disruption of neural information processing in an animal model of schizophrenia.

What mechanism might underlie the increase in SWRs in KO mice? The shift in plasticity away from LTD and toward LTP (Zeng et al., 2001) would suggest an increase in excitability, which may produce an increase in the SWR number. In support, an electrophysiological study of CA1–CA3 slices producing spontaneous SWRs demonstrated that SWR abundance increases after LTP induction, and that this effect is dependent on NMDA receptors (Behrens et al., 2005). Next, how can the plasticity shift in KO mice affect the temporal organization of place cell activity during SWRs? Several models have

proposed that synaptic plasticity occurring during exploratory running behavior may drive associations between successively active place cells, and sculpt the sequences that can be subsequently generated (Jensen and Lisman, 1996; Levy, 1996; Mehta et al., 2002). Synaptic plasticity that is excessive and unbalanced toward potentiation in calcineurin KO might cause excessive temporal binding between place cells during running behavior, despite the fact that the activity of the place cells during running is normal. Hence, this excessive temporal binding would then be manifested during the information retrieval process associated with SWRs.

Our results suggest that information processing during awake resting periods may play a critical role in normal brain function. Recently, there has been increasing interest in resting-state brain function and a related set of brain regions known as the “default mode network” (DMN), including the hippocampal formation as well as posterior cingulate cortex, retrosplenial cortex and prefrontal cortex (Broyd et al., 2009; Buckner et al., 2008; Buckner and Carroll, 2007; Raichle et al., 2001). It has also been proposed that the complex symptoms of schizophrenia could arise from an overactive or inappropriately active DMN (Buckner et al., 2008). For example, within schizophrenia patients, increased DMN activity during rest periods was correlated with the positive symptoms of the disorder (*eg* hallucinations, delusions and thought confusions) (Garrity et al., 2007). In addition, another study reported that DMN regions were correlated with each other to a significantly higher degree in schizophrenia patients compared to controls (Zhou et al., 2007). Here we demonstrated that offline activity in the hippocampus, one of the DMN regions, is disrupted in calcineurin KO mice, thus providing the first evidence for DMN dysfunction in an animal model of schizophrenia.

Our finding that the basic physiological properties of place cells are normal in KO, despite their displaying a range of spatial learning impairments, reinforces the conclusion drawn in many previous studies that place fields *per se* may not provide a robust indicator of spatial learning and memory (McHugh et al., 2007; Nakashiba et al., 2008; Suh et al., 2011). For instance, mice in which the projection from the layer III principal cells of the medial entorhinal cortex to hippocampal area CA1 was specifically blocked by transgenic tetanus toxin displayed normal basic properties of CA1 place fields including field size, mean firing rate, and spatial information, and yet these mice exhibited impairments in spatial working memory (Suh et al., 2011). By contrast, the precise and complete blockade of CA3 input to CA1 by transgenic tetanus toxin resulted in specific deficits both in the SWR frequency and SWR-associated co-reactivation of CA1 cells during sleep, which correlate with a deficit in memory consolidation at the behavioral level (Nakashiba et al., 2009). Likewise, disruption of neural activity during SWRs by electrical micro-stimulation causes learning impairment (Ego-Stengel and Wilson, 2010; Girardeau et al., 2009). These and our present findings add to the growing evidence that more complex aspects of place cell activity, such as SWR-associated features, may be necessary elements of hippocampal information processing for learning and memory (Diba and Buzsaki, 2007; Foster and Wilson, 2006; Jadhav et al., 2012; Nakashiba et al., 2009; Pfeiffer and Foster, 2013; Wilson and McNaughton, 1994). Therefore, disruption of the temporal order of hippocampal place cell spikes during SWRs in KO mice suggests a novel mechanism underlying the cognitive impairments observed in schizophrenia.

The increase in SWR events provide a model that might unify several disparate aspects of schizophrenia: (1) the role of NMDA receptors in schizophrenia (the “glutamate hypothesis” (Olney and Farber, 1995)) which is consistent with altered SWR abundance resulting from an imbalance in NMDA-receptor dependent synaptic plasticity mechanisms; (2) the cognitive symptoms of schizophrenia, which may be accounted for by SWR-mediated disruption of DMN function; (3) the presence of psychosis and disordered thinking in



schizophrenia, which may result from abnormal memory reactivation in cortical areas caused by abnormal memory reactivation in the hippocampus; and (4) abnormalities in dopaminergic signaling (the “dopamine hypothesis” (Carlsson, 1977)), which may result from the effect of increased SWR abundance on downstream dopaminergic circuits (Lansink et al., 2009; Pennartz et al., 2004). Therefore, our findings provide a novel link that SWR activity may constitute a point of convergence across disparate schizophrenia models, and a new insight into the neural basis of the cognitive disorder.

## EXPERIMENTAL PROCEDURES

### Mouse Breeding

To obtain the conditional knockout (KO) mice, we followed the breeding paradigm published previously (Zeng et al, 2001). Briefly, female homozygous for the floxed CNB (fCN) allele and carrying the aCaMKII-Cre transgene was crossed to male homozygous fCN to produce KO and littermate fCN control (CT). All mice were maintained in a pure C57BL/6 background and housed in a room with a 12-hr light/dark cycle (light on at 7 am) with access to food and water *ad libitum*. Tail DNA was collected to identify the genotypes of animals using PCR. All procedure relating to animal care and treatment conformed to the Institutional and NIH guidelines.

### In vivo recording

Male mice (KO and CT) between 12–16 weeks of age were anesthetized i.p. with avertin (300 mg/kg, 1.25% solution) and implanted with a microdrive hosting six independently adjustable tetrodes. The tetrode tips were gold-plated before surgery in order to reduce impedances to 200–250 kOhms (AP –1.8 mm, ML 1.6 mm) to aim for dorsal CA1. The microdrive was secured to the skull using watch screws and dental cement and a screw fixed to the skull served as a ground electrode. The tetrodes were lowered over 10–14 days in steps of 40  $\mu$ m until ripple and the hippocampal units could be identified. One designated electrode was targeted to the white matter above hippocampus to record a reference signal. Recorded unit signals were amplified 8 k to 20 k times and high-pass filtered above 6 kHz, whereas EEG signals from the same tetrodes were amplified 5 k times and band-pass filtered between 1 and 475 Hz. The animal’s position was tracked with a 30 frames/sec camera using a pair of infrared diodes attached to the animal’s head. Hippocampal activity was recorded using a 16-channel Neuralynx recording system, (Neuralynx, Bozeman, MT) while mice were in either a square enclosure (17  $\times$  17  $\times$  17 cm; “sleep box”), or a linear track (76  $\times$  10 cm). The recording session consisted of one “RUN” epoch on the track (40–60 min) bracketed by two “SLEEP” epochs (30–60 min) in which the animal rested quietly in the sleep box in the same room. Following the recording session, manual clustering of spikes was done with XCLUST2 software (developed by M.A. Wilson, MIT). At the end of the experiment, mice were given a lethal dose of avertin and an electric current (50 mA) was delivered to create a small lesion at the tip of each tetrode. Animals were then transcardially perfused with 4% paraformaldehyde in 1 x phosphate-buffered saline and brains were removed, sliced in 50  $\mu$ m with a Vibratome, and mounted on slides to verify the recording positions. All experiments were conducted and analyzed by researchers blind to the genotype of the individual animals.

### Neural data analysis

**Ripple analysis**—One electrode from each tetrode that had at least one cluster was considered for EEG analysis. EEG signal of each electrode was denoised for 60 Hz electric noise and its 180 Hz harmonic using a second-order IIR notch filter. Denoised EEG was filtered at ripple frequency range (100–240 Hz) with a fifth-order Butterworth band-pass filter. The envelopes of each band-passed EEG were obtained using the absolute value of its

Hilbert transform and these envelopes were averaged over all electrodes. After applying a Gaussian smoother with 5 ms standard deviation, the averaged envelope was z-scored. Events that passed 5 standard deviations (i.e. mean + 5 sd of averaged non-z-scored envelope) for more than 3 ms were considered as ripples, and ripples that were less than 20 ms apart were merged and were considered as one extended ripple. The beginning and end of each ripple were considered as where the smoothed envelope crossed its mean value (i.e. zero for z-scored signal). Ripples events that happened when mice were not immobilized were excluded. Mice were considered as immobilized when their head speed was below 0.5 cm/s. Ripple power was obtained by applying Welch's method on each individual non-z-scored non-enveloped ripples and then averaging over calculated powers. Morlet wavelet scalogram with bandwidth of 10 was used for spectrogram visualization of raw EEG. The same ripple-finding algorithm was also applied for gamma frequency range (25–80 Hz), to investigate if the impairment in EEG power is only selective for ripple events or can be found in gamma activity when animal is in immobilized state. Also, using Welch's method, the power of raw EEG signals during run was calculated and, in particular, theta (4–12 Hz) powers for CT and KO mice were compared. For a robustness analysis, EEGs were filtered with 50-Hz-wide frequency filters ranging from 50 Hz to 600 Hz with 40 Hz overlap between two consecutive filters.

**Cluster analysis**—Manual clustering of spikes was done based on spike waveform peak amplitude using XCLUST2 software (M.A. Wilson, MIT). Putative interneurons were also excluded from analysis on the basis of their spike width. To compare the quality of clusters in mice genotypes a modified  $L_{ratio}$  value for each cluster of a tetrode was calculated (Pfeiffer and Foster, 2013; Schmitzer-Torbert et al., 2005):

$$L_{ratio} = \left( \sum_{i \notin C} \left( 1 - CDF_{\chi^2_{df}}(D_{i,C}^2) \right) \right) / n_s$$

where  $i \notin C$  is the set of spikes that do not belong to target cluster C and  $D_{i,C}$  is the Mahalanobis distance of these spikes from this cluster.  $CDF_{\chi^2_{df}}$  is the cumulative distribution function of  $\chi^2$  distribution with  $df = 4$  (feature space for clusters is four dimensional).  $n_s$  is the total number of spikes from all the clusters (including target cluster C) of the tetrode.

**Place cell analysis**—All the place cell analyses, except spatial coherence, were done on 1-D place fields. These 1-D place fields were obtained by using 2 cm bins on linear track, and these raw place fields were smoothed by applying a Gaussian smoother with a 2.4 cm standard deviation. Place field size was calculated as the number of 2-cm-wide bins above 1 Hz threshold. Directionality index of each place field was defined as the percentage of its dominant direction (the direction that a specific cell has higher peak firing) divided by the summation of both left and right firings. Sparsity index ranges from 0 to 1, while less value means a less diffuse and more spatially specific place field (Markus et al., 1994). Having  $n$  two-cm bins ( $n=38$ ) each having firing rate of  $f_i$  and occupancy time of  $t_i$ , we would have:

$$\text{Sparsity} = \frac{(\sum_{i=1}^n p_i \cdot f_i)^2}{\sum_{i=1}^{38} p_i \cdot f_i^2}$$

where  $p_i$  is the occupancy probability:  $p_i = t_i / \sum_{i=1}^n t_i$  Spatial information which is the amount of information about animal's position by each spike of a place cell is calculated as follows (Markus et al., 1994):

$$\text{Spatial Information} = \sum_{i=1}^n p_i \frac{f_i}{f} \log_2 \frac{f_i}{f}$$

where  $f = \sum_{i=1}^n p_i f_i$  is the mean firing rate.

Spatial coherence which quantifies smoothness and local orderliness of a place field is the autocorrelation of each 2-D place field with its nearest neighbor average (Muller and Kubie, 1989). To do this, 10×70 cm linear track was binned to 2 cm × 2 cm bins and the new firing map for each pixel was calculated as the average firing rate of 8 unsmoothed neighbor pixels. Then, 2-D correlation coefficient between original unsmoothed firing map and the new one was calculated and to be statistically more meaningful this coefficient became Fisher-transformed (z-transformed).

For visualization purpose, 2-D place fields were calculated using 1×1 cm bins smoothed with a 1-cm standard deviation Gaussian smoother.

**Burst analysis**—For each place cell spikes that happened in less than 10 ms apart during run were considered as in-burst spikes. For each burst, amplitude difference was defined as the average of the change in peak of new spike waveform in relation to previous spike waveform. These calculated values were averaged over all bursts and using ISI of in-burst spikes, each cell was able to be shown as one point in a 2-D (amplitude difference versus ISI) feature space.

**Reactivation analysis**—For each ripple, spikes happening from 300 ms before it to 300 ms after it were considered as ripple-associated spikes, and cells with at least one spike in one ripple were called “active cells”. Only these ripple-associated spikes were considered for calculation of pair-wise cross-correlogram. For each pair of cells the histograms of these spikes were calculated in 5 ms bins. Each histogram was smoothed with a 5-sample moving-average smoother. Then, cross-correlation of this pair of smoothed histograms was calculated. Calculation was performed for all the cell-pairs for each mouse and averaged over the cell-pairs that their place field peaks fall within same 3-cm-binned distance. The, these cross-correlograms were averaged and normalized for all mice in different genotypes and shown only for visualization purpose. However, for statistical analysis of reactivation, the average of spike timing of each pair was calculated. Knowing the place field distance of all pairs, each pair becomes a point in a 2-D (spike separation versus place field distance) coordinate space. Regression was used to fit these points, and the amount of correlation and its statistical significance measured the extent to which pairs of cells with spatially separated fields fired at longer temporal separations during ripples, compared with pairs of cells with spatially proximal fields. To further confirm this, pair cells with less 10 cm distance between their place fields were considered as “close” cells while cells with more than 40 cm distance were considered as “far” cells. The average relative spike timing of these “close” and “far” cells was calculated for each genotype.

Furthermore, to directly comparing pairs between CT and KO, a 3-way nested analysis of variance (ANOVA) was used which considered distance between pairs (“far” versus “close”) and genotypes (CT versus KO) as fixed-effect factors, and mice as a random-effect factor nested in genotypes. To investigate if the mean of correlation coefficients across animals is significantly different in CT versus KO we use z-test. To be statistically comparable we applied a Fisher transform (or z-transform,  $z = \text{arctanh}(r)$ ) on correlation coefficients before calculating Z-values.

## Supplementary Material

Refer to Web version on PubMed Central for supplementary material.

## Acknowledgments

The work was supported by RIKEN Brain Science Institute (to S.T.), NIH grants MH78821 (to S.T.), MH58880 (to S.T.), MH086702 (to D.J.F.), Alfred P. Sloan Research Fellowship (to D.J.F.), NARSAD Young Investigator Award (to D.J.F.), and Johns Hopkins Brain Science Institute (to D.J.F.).

## References

- Arguello PA, Gogos JA. Modeling madness in mice: one piece at a time. *Neuron*. 2006; 52:179–196. [PubMed: 17015235]
- Behrens CJ, van den Boom LP, de Hoz L, Friedman A, Heinemann U. Induction of sharp wave-ripple complexes in vitro and reorganization of hippocampal networks. *Nat Neurosci*. 2005; 8:1560–1567. [PubMed: 16222227]
- Broyd SJ, Demanuele C, Debener S, Helps SK, James CJ, Sonuga-Barke EJ. Default-mode brain dysfunction in mental disorders: a systematic review. *Neurosci Biobehav Rev*. 2009; 33:279–296. [PubMed: 18824195]
- Buckner RL, Andrews-Hanna JR, Schacter DL. The brain's default network: anatomy, function, and relevance to disease. *Ann N Y Acad Sci*. 2008; 1124:1–38. [PubMed: 18400922]
- Buckner RL, Carroll DC. Self-projection and the brain. *Trends Cogn Sci*. 2007; 11:49–57. [PubMed: 17188554]
- Buzsaki G. Two-stage model of memory trace formation: a role for “noisy” brain states. *Neuroscience*. 1989; 31:551–570. [PubMed: 2687720]
- Carlsson A. Does dopamine play a role in schizophrenia? *Psychological medicine*. 1977; 7:583–597. [PubMed: 22890]
- Davidson TJ, Kloosterman F, Wilson MA. Hippocampal replay of extended experience. *Neuron*. 2009; 63:497–507. [PubMed: 19709631]
- Diba K, Buzsaki G. Forward and reverse hippocampal place-cell sequences during ripples. *Nat Neurosci*. 2007; 10:1241–1242. [PubMed: 17828259]
- Dragoi G, Tonegawa S. Preplay of future place cell sequences by hippocampal cellular assemblies. *Nature*. 2011; 469:397–401. [PubMed: 21179088]
- Dragoi G, Tonegawa S. Distinct preplay of multiple novel spatial experiences in the rat. *Proc Natl Acad Sci U S A*. 2013; 110:9100–9105. [PubMed: 23671088]
- Dudek SM, Bear MF. Homosynaptic long-term depression in area CA1 of hippocampus and effects of N-methyl-D-aspartate receptor blockade. *Proc Natl Acad Sci U S A*. 1992; 89:4363–4367. [PubMed: 1350090]
- Ego-Stengel V, Wilson MA. Disruption of ripple-associated hippocampal activity during rest impairs spatial learning in the rat. *Hippocampus*. 2010; 20:1–10. [PubMed: 19816984]
- Ekstrom AD, Kahana MJ, Caplan JB, Fields TA, Isham EA, Newman EL, Fried I. Cellular networks underlying human spatial navigation. *Nature*. 2003; 425:184–188. [PubMed: 12968182]
- Elvevag B, Goldberg TE. Cognitive impairment in schizophrenia is the core of the disorder. *Critical reviews in neurobiology*. 2000; 14:1–21. [PubMed: 11253953]
- Foster DJ, Wilson MA. Reverse replay of behavioural sequences in hippocampal place cells during the awake state. *Nature*. 2006; 440:680–683. [PubMed: 16474382]
- Gaffan D. Scene-specific memory for objects - a model of episodic memory impairment in monkeys with fornix transection. *J Cognitive Neurosci*. 1994; 6:305–320.
- Garrity AG, Pearlson GD, McKiernan K, Lloyd D, Kiehl KA, Calhoun VD. Aberrant “default mode” functional connectivity in schizophrenia. *The American journal of psychiatry*. 2007; 164:450–457. [PubMed: 17329470]
- Gerber DJ, Hall D, Miyakawa T, Demars S, Gogos JA, Karayiorgou M, Tonegawa S. Evidence for association of schizophrenia with genetic variation in the 8p21.3 gene, PPP3CC, encoding the

- calcineurin gamma subunit. *Proc Natl Acad Sci U S A*. 2003; 100:8993–8998. [PubMed: 12851458]
- Gerber DJ, Tonegawa S. Psychotomimetic effects of drugs--a common pathway to schizophrenia? *The New England journal of medicine*. 2004; 350:1047–1048. [PubMed: 14999118]
- Girardeau G, Benchenane K, Wiener SI, Buzsaki G, Zugaro MB. Selective suppression of hippocampal ripples impairs spatial memory. *Nat Neurosci*. 2009; 12:1222–1223. [PubMed: 19749750]
- Goldman-Rakic PS. Working memory dysfunction in schizophrenia. *The Journal of neuropsychiatry and clinical neurosciences*. 1994; 6:348–357. [PubMed: 7841806]
- Gupta AS, van der Meer MA, Touretzky DS, Redish AD. Hippocampal replay is not a simple function of experience. *Neuron*. 2010; 65:695–705. [PubMed: 20223204]
- Harris KD, Hirase H, Leinekugel X, Henze DA, Buzsaki G. Temporal interaction between single spikes and complex spike bursts in hippocampal pyramidal cells. *Neuron*. 2001; 32:141–149. [PubMed: 11604145]
- Harrison BJ, Yucel M, Pujol J, Pantelis C. Task-induced deactivation of midline cortical regions in schizophrenia assessed with fMRI. *Schizophrenia research*. 2007; 91:82–86. [PubMed: 17307337]
- Jadhav SP, Kemere C, German PW, Frank LM. Awake hippocampal sharp-wave ripples support spatial memory. *Science*. 2012; 336:1454–1458. [PubMed: 22555434]
- Jensen O, Lisman JE. Hippocampal CA3 region predicts memory sequences: accounting for the phase precession of place cells. *Learning and Memory*. 1996; 3:279–287. [PubMed: 10456097]
- Jung MW, Wiener SI, McNaughton BL. Comparison of spatial firing characteristics of units in dorsal and ventral hippocampus of the rat. *J Neurosci*. 1994; 14:7347–7356. [PubMed: 7996180]
- Karlsson MP, Frank LM. Awake replay of remote experiences in the hippocampus. *Nat Neurosci*. 2009; 12:913–918. [PubMed: 19525943]
- Lansink CS, Goltstein PM, Lankelma JV, McNaughton BL, Pennartz CM. Hippocampus leads ventral striatum in replay of place-reward information. *PLoS Biol*. 2009; 7:e1000173. [PubMed: 19688032]
- Levy WB. A sequence predicting CA3 is a flexible associator that learns and uses context to solve hippocampal-like tasks. *Hippocampus*. 1996; 6:579–590. [PubMed: 9034847]
- Markus EJ, Barnes CA, McNaughton BL, Gladden VL, Skaggs WE. Spatial information content and reliability of hippocampal CA1 neurons: effects of visual input. *Hippocampus*. 1994; 4:410–421. [PubMed: 7874233]
- Matsumura N, Nishijo H, Tamura R, Eifuku S, Endo S, Ono T. Spatial- and task-dependent neuronal responses during real and virtual translocation in the monkey hippocampal formation. *J Neurosci*. 1999; 19:2381–2393. [PubMed: 10066288]
- McHugh TJ, Blum KI, Tsien JZ, Tonegawa S, Wilson MA. Impaired hippocampal representation of space in CA1-specific NMDAR1 knockout mice. *Cell*. 1996; 87:1339–1349. [PubMed: 8980239]
- McHugh TJ, Jones MW, Quinn JJ, Balthasar N, Coppari R, Elmquist JK, Lowell BB, Fanselow MS, Wilson MA, Tonegawa S. Dentate gyrus NMDA receptors mediate rapid pattern separation in the hippocampal network. *Science*. 2007; 317:94–99. [PubMed: 17556551]
- Mehta MR, Lee AK, Wilson MA. Role of experience and oscillations in transforming a rate code into a temporal code. *Nature*. 2002; 417:741–746. [PubMed: 12066185]
- Miyakawa T, Leiter LM, Gerber DJ, Gainetdinov RR, Sotnikova TD, Zeng H, Caron MG, Tonegawa S. Conditional calcineurin knockout mice exhibit multiple abnormal behaviors related to schizophrenia. *Proc Natl Acad Sci U S A*. 2003; 100:8987–8992. [PubMed: 12851457]
- Morris RG, Garrud P, Rawlins JN, O'Keefe J. Place navigation impaired in rats with hippocampal lesions. *Nature*. 1982; 297:681–683. [PubMed: 7088155]
- Muller RU, Kubie JL. The firing of hippocampal place cells predicts the future position of freely moving rats. *J Neurosci*. 1989; 9:4101–4110. [PubMed: 2592993]
- Nakashiba T, Buhl DL, McHugh TJ, Tonegawa S. Hippocampal CA3 output is crucial for ripple-associated reactivation and consolidation of memory. *Neuron*. 2009; 62:781–787. [PubMed: 19555647]



- Nakashiba T, Young JZ, McHugh TJ, Buhl DL, Tonegawa S. Transgenic inhibition of synaptic transmission reveals role of CA3 output in hippocampal learning. *Science*. 2008; 319:1260–1264. [PubMed: 18218862]
- O'Keefe J, Dostrovsky J. The hippocampus as a spatial map. Preliminary evidence from unit activity in the freely-moving rat. *Brain Res*. 1971; 34:171–175. [PubMed: 5124915]
- O'Keefe, J.; Nadel, L. The hippocampus as a cognitive map. Oxford University Press; 1978.
- Olney JW, Farber NB. Glutamate receptor dysfunction and schizophrenia. *Archives of general psychiatry*. 1995; 52:998–1007. [PubMed: 7492260]
- Olton DS, Samuelson RJ. Remembrance of places passed: spatial memory in rats. *J Exp Psychol Anim Behav Process*. 1976; 2:97–116.
- Pennartz CM, Lee E, Verheul J, Lipa P, Barnes CA, McNaughton BL. The ventral striatum in off-line processing: ensemble reactivation during sleep and modulation by hippocampal ripples. *J Neurosci*. 2004; 24:6446–6456. [PubMed: 15269254]
- Quirk MC, Wilson MA. Interaction between spike waveform classification and temporal sequence detection. *J Neurosci Methods*. 1999; 94:41–52. [PubMed: 10638814]
- Pfeiffer BE, Foster DJ. Hippocampal place-cell sequences depict future paths to remembered goals. *Nature*. 2013; 497:74–79. [PubMed: 23594744]
- Raichle ME, MacLeod AM, Snyder AZ, Powers WJ, Gusnard DA, Shulman GL. A default mode of brain function. *Proc Natl Acad Sci U S A*. 2001; 98:676–682. [PubMed: 11209064]
- Schmitzer-Torbert N, Jackson J, Henze D, Harris K, Redish AD. Quantitative measures of cluster quality for use in extracellular recordings. *Neuroscience*. 2005; 131:1–11. [PubMed: 15680687]
- Scoville WB, Milner B. Loss of recent memory after bilateral hippocampal lesions. *Journal of neurology, neurosurgery, and psychiatry*. 1957; 20:11–21.
- Skaggs WE, McNaughton BL, Wilson MA, Barnes CA. Theta phase precession in hippocampal neuronal populations and the compression of temporal sequences. *Hippocampus*. 1996; 6:149–172. [PubMed: 8797016]
- Small SA, Schobel SA, Buxton RB, Witter MP, Barnes CA. A pathophysiological framework of hippocampal dysfunction in ageing and disease. *Nat Rev Neurosci*. 2011; 12:585–601. [PubMed: 21897434]
- Steele RJ, Morris RG. Delay-dependent impairment of a matching-to-place task with chronic and intrahippocampal infusion of the NMDA-antagonist D-AP5. *Hippocampus*. 1999; 9:118–136. [PubMed: 10226773]
- Suh J, Rivest AJ, Nakashiba T, Tominaga T, Tonegawa S. Entorhinal cortex layer III input to the hippocampus is crucial for temporal association memory. *Science*. 2011; 334:1415–1420. [PubMed: 22052975]
- Weinberger DR. Cell biology of the hippocampal formation in schizophrenia. *Biol Psychiatry*. 1999; 45:395–402. [PubMed: 10071707]
- Wilson MA, McNaughton BL. Dynamics of the hippocampal ensemble code for space. *Science*. 1993; 261:1055–1058. [PubMed: 8351520]
- Wilson MA, McNaughton BL. Reactivation of hippocampal ensemble memories during sleep. *Science*. 1994; 265:676–679. [PubMed: 8036517]
- Zeng H, Chattarji S, Barbarosie M, Rondi-Reig L, Philpot BD, Miyakawa T, Bear MF, Tonegawa S. Forebrain-specific calcineurin knockout selectively impairs bidirectional synaptic plasticity and working/episodic-like memory. *Cell*. 2001; 107:617–629. [PubMed: 11733061]
- Zhou Y, Liang M, Tian L, Wang K, Hao Y, Liu H, Liu Z, Jiang T. Functional disintegration in paranoid schizophrenia using resting-state fMRI. *Schizophrenia research*. 2007; 97:194–205. [PubMed: 17628434]

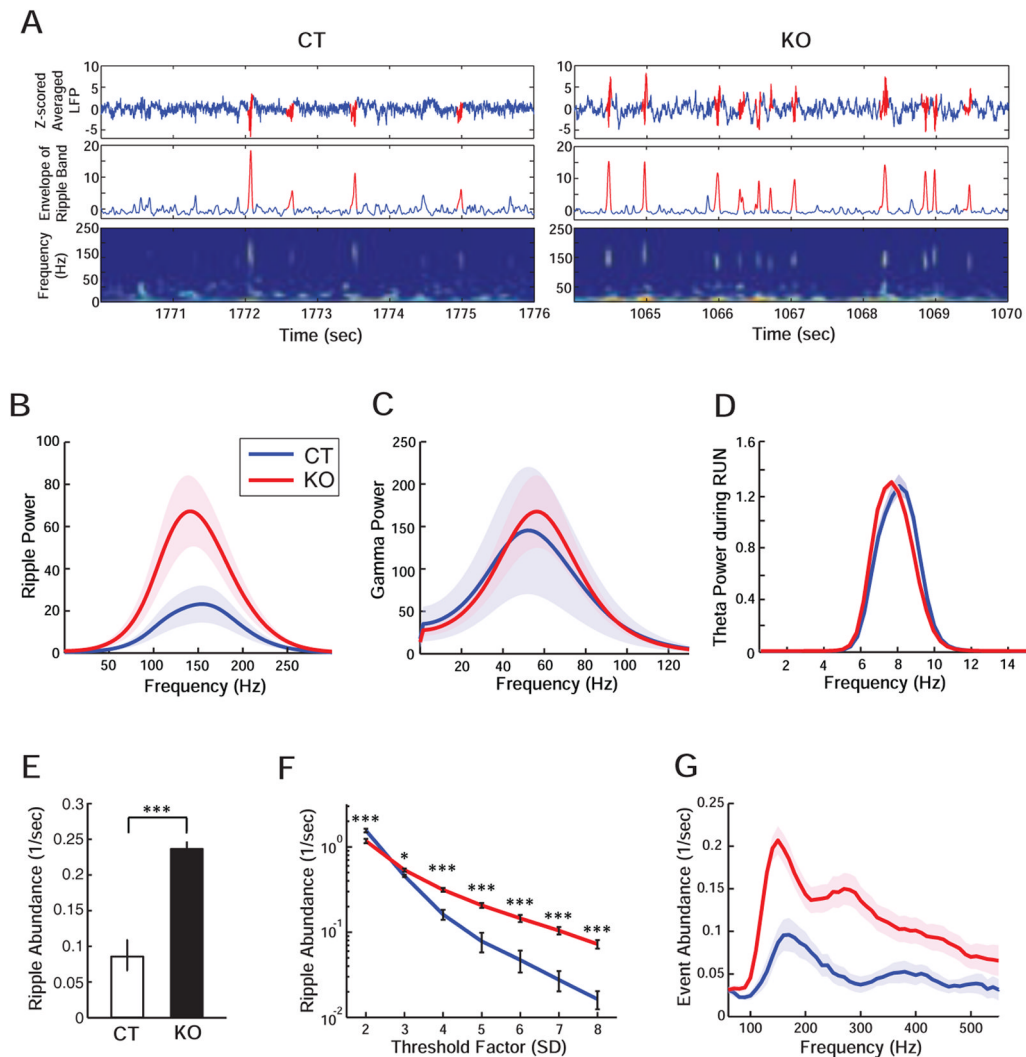


**Figure 1. Increased hippocampal ripple activity in calcineurin KO mice during awake resting periods**

(A) Examples of EEG recording from CT (left) and KO (right) mice. Each EEG trace is shown as z-scored raw EEG (top), envelope of smoothed ripple-band-filtered EEG (middle) and wavelet power spectrogram of raw EEG (bottom). Note that sharp waves and their associated ripples are clearly isolated events in this spectrogram. (B–C) Comparison of spectral power of EEG filtered at ripple (B, 100–240 Hz) and gamma (C, 25–80 Hz) frequency bands, in both cases for EEG. (D) Comparison of spectral power of z-scored raw EEG filtered at theta (4–12 Hz) band during run. (E) Comparison of ripple abundance during awake resting period. (F) Quantitative measurement of ripple abundance at different threshold factors (standard deviations of z-scored, smoothed and filtered EEG). (G) The abundance of EEG events measured by a 50 Hz frequency window that filtered raw EEG at different frequency bands. Data are represented as mean  $\pm$  SEM (shaded area in B, C, D and G).

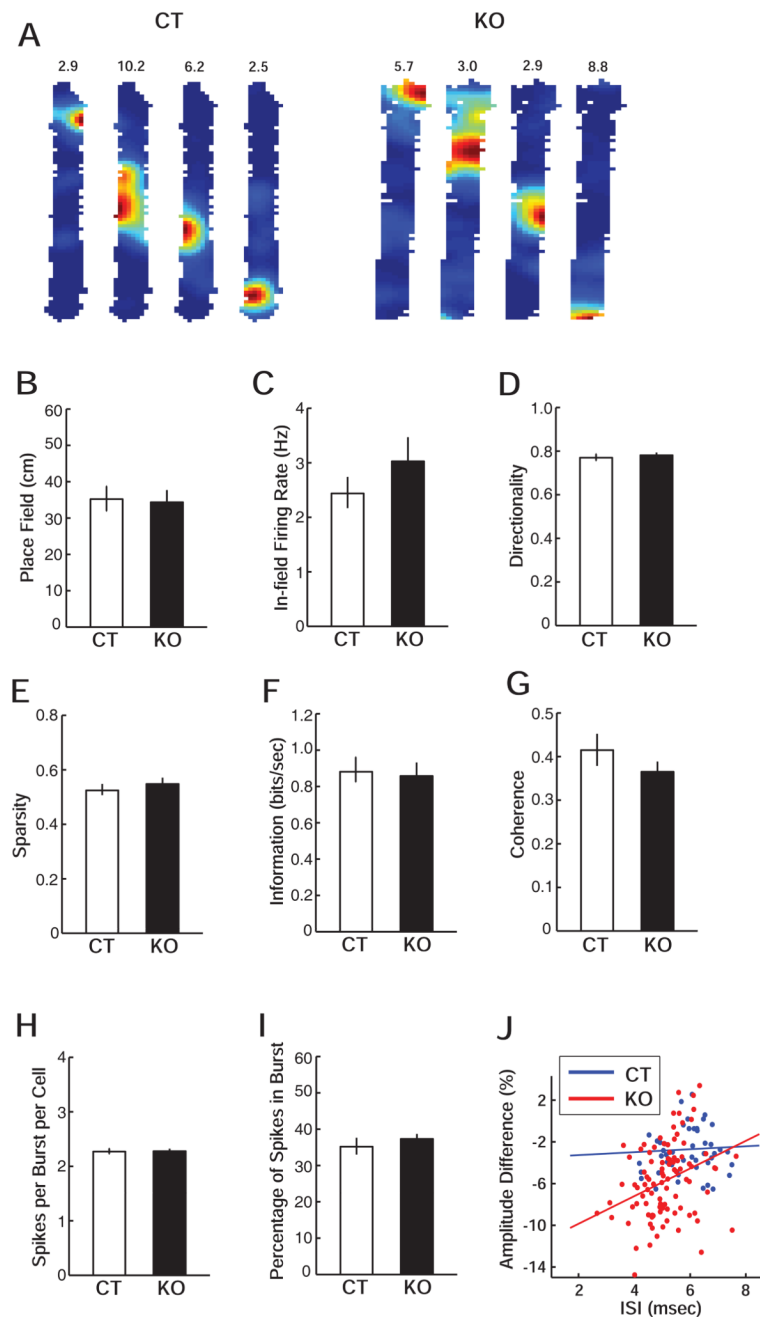


**Figure 2. Similar basic properties of place cells in CT and KO mice in run periods**

(A) Examples of color-coded firing rate maps of CA1 place cells during run on a  $10 \times 76$  cm linear track. Peak firing rates in Hz are shown above each rate map. (B–G) Quantitative description of place fields of CT and KO mice: (B) size of place field, (C) mean in-field firing rate, (D) directionality, (E) sparsity, (F) spatial information, and (G) spatial coherence. (H–J) Quantification of spike activity during burst: (H) number spikes per burst per cell, and (I) the proportion of spikes, which were burst spikes, per cell. Data are represented as mean  $\pm$  SEM. (J) The percentage of attenuation in spike amplitude within bursts as a function of in-burst inter-spike interval (ISI) for each cell (CT: 48 cells; KO: 97 cells).

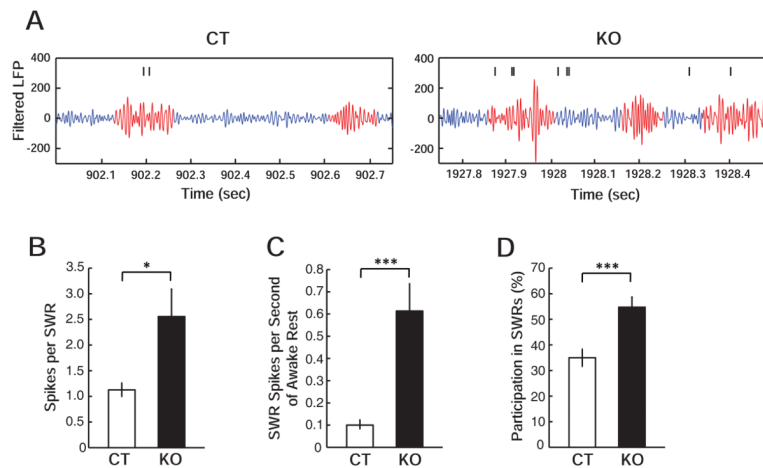


**Figure 3. Increased spike activity of place cells in calcineurin KO mice during ripple events** (A) A representative train of spikes is displayed with simultaneously recorded EEG filtered in ripple frequency range, for CT and KO. Ripple events are highlighted in red. (B) The number of spikes per SWR event, per cell (over all cells that fired at least one spike during at least one SWR event). (C) The number of SWR spikes per second of awake resting period, per cell. (D) The fractional participation in SWRs, i.e., the fraction of SWR events for which a cell fired at least one spike, averaged across all cells. Data are represented as mean  $\pm$  SEM.

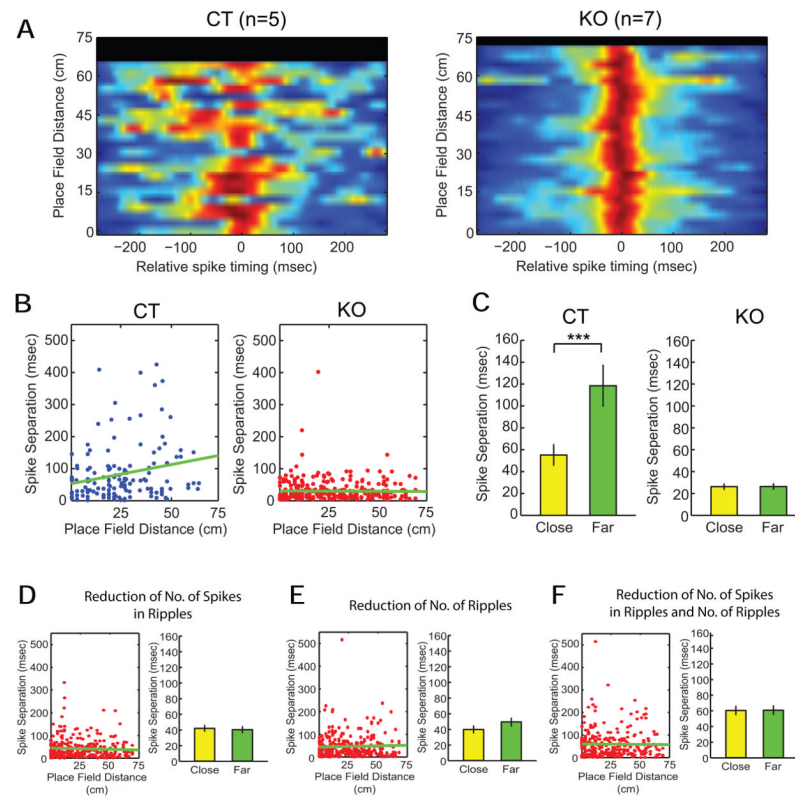


**Figure 4. Impaired reactivation of spatial experience on the linear track during awake resting periods on the linear track in calcineurin KO mice**

(A) For each pair of neurons, the pairwise cross-correlogram of the two spike trains around ripple events ( $\pm 300$  ms) is plotted at a y position given by the linear distance between the corresponding two place field peaks. Wherever more than one pair occupies the same y position (*ie* has the same inter-peak spatial distance), the cross-correlograms have been averaged. Pairwise data from all sessions are shown together on the left for CT and on the right for KO. (B) Distribution of temporal spike separations during ripples of all pairs of neurons is plotted as a function of the distance between place field peaks on the track. (C) Comparison of the average spike separation for pairs of cells with place field peaks less than 10 cm apart (close cells) and pairs of cells with place field peaks more than 40 cm apart (far cells). (D–F) For KO mice, the reactivation assessment shown in (B) was reanalyzed while only extra spikes (D), only extra ripples (E), or both extra spikes and ripples (F) were randomly decimated. Data are represented as mean  $\pm$  SEM.